*Desalination and Water Treatment*
www.deswater.com

doi: 10.5004/dwt.2017.0118

60 (2017) 48–57
January

# The integration of humidification dehumidification desalination and flue gas desulfurization

Nagla F. Attia

*Water Research Center, Kuwait Institute for scientific Research, P.O. Box 24885, Safat 13109, Kuwait, emails: nagla.attia@yahoo.com, nattia@kisr.edu.kw*

Received 29 January 2016; Accepted 18 May 2016

**ABSTRACT**

This study was focused on modeling of the integration system of flue gas desulfurization (FGD) and humidification dehumidification desalination (HDD). The study dealt with the development of appropriate models for two alternative process flow structures intended for achieving the target of FCO by seawater while obtaining a fresh water credit. Each of the two schemes was dealt with separately. This included a brief description of the characteristic features of each scheme, models associated with the formulation of overall mass and heat balances, and the design equations used for rating the various components within each process scheme. The proposed model was applied to the operating conditions of the power plants in Kuwait, motivated by the large capacity of these plants and the use of high sulfur oil fuels. The analysis included sizing of the required HDD units, evaluation of the specific amounts of water generated relative to the plant power capacity, the design characteristics, and the performance of the flue gas/seawater heat exchanger and seawater absorption column for sulfur dioxide removal from the flue gases. The two alternative configurations were compared by summarizing the results of the major factors affecting the initial and operating costs associated with the different schemes.

*Keywords:* Flue gas desulfurization; Humidification; Dehumidification; Desalination

## 1. Introduction

With the rapidly growing world population and burgeoning economic development across much of the world, issues of energy security and environmental degradation will likely grow increasingly prominent in national agendas. Achieving solutions will not be easy, but enhancing energy security and averting future harms to the environment is possible, and can be profitable. Therefore, it is important to devise methods for reducing the flue gas emissions generated by the combustion of fossil fuels, which have severe effects on the local, downwind, and global environment. To reduce dependence and demand on fossil fuels, governments, businesses, and individuals can develop fossil fuel energy alternatives, increase energy efficiency, and reduce energy consumption [1].

Energy consumption in Kuwait is increasing annually by 8%. The major energy consumption is from power plant. Alotaibi [2] estimated that the energy consumption in Kuwait power plants would reach 26.5% of the total oil produced by the year 2020. As per oil production rate in 2008, the energy produced will be consumed locally by the year 2027. Unfortunately, fossil fuel used in power plant contains high sulfur which contributes to air pollution. Several researchers had investigation on the air pollution related to power generation in Kuwait. Darwish and Al-Wajan [3] reviewed the status of the power plant capacities and limitations of the currently available facilities in satisfying increasing demand in electricity in Kuwait. Their study suggested a mechanism to increase the electricity production efficiency instead of building new plants. Previously, Darwish et al. [4] discussed the sustainability of energy and desalted water and their impact on the environment. They also mentioned some

* Corresponding author.

1944-3994/1944-3986 © 2017 Desalination Publications. All rights reserved.

energy-efficient methods for the desalination plants to conserve energy based on an energy analysis. Models of energy consumption in Kuwait and several sophisticated models are available. Recently, Alhaddad et al. [5] analyzed the air pollution emission in the vicinity of oil refineries. The emission data obtained for oil refineries are used to predict the pollutant concentrations using the AERMOD software and ISCST model. The results showed that the strongest contribution to air pollution comes from oil field, power plant, and traffic.

The exploitation of the heat rejected to environment by a steam power cycle for seawater distillation is a consolidated practice in the desalination industry through several dual-purpose installations, especially in the Middle East where typically, the steam discharged by a backpressure steam turbine feeds the brine heater of a multi stage flash (MSF) distiller. Cohen et al. [6] assessed two methods for utilizing the waste heat of the flue gases from coal-fired power plant as a heat source in a multi-effect distillation (MED) plant. They concluded that 8,500–10,000 $m^3 d^{-1}$ of high-quality water (~10 mg $l^{-1}$ total dissolved solids (TDS)) may be produced from one 575-MW generating unit. Moreover, a great amount of water is saved due to reduction in flue gas temperature and simultaneously a reduction in water evaporation in the flue gas scrubber. The water cost obtained is in the range of US 53–62 cent $m^{-3}$, depends on the MED, gas cooler capital costs, unit capacity factor, and required rate of return. The obtained costs are comparable to water cost obtained from state-of-threat, large-scale seawater reverse osmosis (SWRO) plants even without taking into account the higher water quality. In addition, Cohen et al. [7] investigated a way of exploiting for seawater distillation the waste heat as rejected by an existing condensation steam power cycle, where only a few degrees are above ambient temperature, without detriment to the electric output of the power station. The study carried out for small-scale units was devoted to boiler make-up production, and for a large plant able to produce the whole water supply for the site. The investigation showed very interesting perspectives for such an application, with extremely low steam, electrical consumption, and a very competitive cost of produced water. Other advantages of low temperature flash technology are related to the extreme plant availability, the high purity of produced distillate, the absence of any chemical consumption, and environmental impact.

## 2. Humidification dehumidification desalination (HDD)

A noticeable interest in HDD technology has emerged during the last decade. HDD has several advantages such as; operating at low temperature (<80°C) and near-ambient pressures, required minimum technical features, low-cost materials, and integration with renewable energy, i.e., solar or wind. HDD represents comparatively new desalination technology based on heat and mass-transfer processes. HDD processes include the following:

- The seawater is converted to water vapor by evaporation into dry air in the evaporator (humidification).
- Water vapor is then condensed out from the air in a condenser to produce freshwater (dehumidification).

Ettouney [8] studied and analyzed the characteristics of our different configurations for the HDD process. The study evaluated the main problems of air humidification dehumidification system, caused by the presence of a large amount of air together with the water vapor product. As a consequence, the efficiency of HDD process is decreased. Al-Enezi et al. [9] measured and analyzed the performance characteristics of the HDD system at low operating temperatures. The measurements showed variations in the production rate which is affected by the hot and cooling water temperatures. The highest production rates are obtained at high hot water temperature, low cooling water temperature, high air flow rate, and low hot water flow rate. The main advantage for low temperature operation is the cost savings related to the capital of the feed water heating device, i.e., the solar collector, electric, or steam heater. Recently, Ettouney et al. [10] studied and analyzed the FGD and HDD of flue gases emitted from power plants in Kuwait. The main feature of the study was to separate the FGD and HDD systems and operate the FGD at low temperatures to maximize sulfur dioxide ($SO_2$) removal while operating the HDD at high temperature to obtain the largest amount of freshwater. The study of the FGD system showed high sensitivity in variations in the height of the absorption column to the removal rate of $SO_2$ and the absorption factor (AF), but the height of the absorption column is less sensitive to variation in the equilibrium constant and diameter of the column. The results of the design data of all power plants in Kuwait showed feasible height for the absorption column which varies between 8.1 and 12.6 m as the power capacity is increased from 244 to 4,173 MW to operate at higher pressure.

Capitalizing on the aforementioned, this study has proposed a system to integrate FGD and HDD. Desalination is based on the exploitation of the relatively high flue gas temperature. The main features of the suggested process are to fulfill the desulphurization requirements of low temperature, while exploiting the relatively high temperature of the flue gases for HDD. Two alternative schemes were proposed, modeled and compared for the integration between FGD and seawater desalination. The process design calculations were based on reliable overall heat and mass transfer coefficient data. In addition, a laboratory scale preliminary set of experiments by Al-Enezi et al. [11] were compared with available data on the mass transfer coefficients for $SO_2$ absorption in seawater and the overall heat transfer coefficients in packed air humidification contacting towers.

## 3. Design and operating parameters

### 3.1. Input conditions

The basis of all calculations was taken as 1,000 kg dry flue gas/h, corresponding to a total flue gas rate of 1110.314 kg $h^{-1}$, having a molecular weight of 27.5604 at 150°C. Table 1 shows a typical analysis of the various flue gas components leaving the economizer. It is clear from Table 1 that the flue gas humidity was calculated as 0.110314 kg water/kg flue gas. Seawater was assumed at a maximum summer temperature of 30°C in the Arabian Gulf. The overall TDS concentration of seawater was taken as 0.047 kg salt/kg salt free water.

### 3.2. Physicochemical parameters

Since the involved salt concentrations are quite small, the vapor pressure of water over the seawater solutions in the

humidification columns was assumed equal to that of freshwater. This enabled the use of standard vapor pressure data available in the literature. The saturation humidity of the air-flue gas systems was based on the average molecular weight of the dry gas stream obtained from the aforementioned standard analysis ($M_g$ = 29.27571). This corresponds to a density of about 1.2 kg $m^{-3}$ (NTP). The specific heat temperatures of the gas $C_g$ and vapor $C_w$ were taken, respectively, at 0.24 and 0.45 kcal $kg^{-1}$.°C, while the latent heat of vaporization λ was taken, at 597.33 kcal $kg^{-1}$ at 0°C. The specific heat of seawater within the operating concentration range was assumed for simplicity to be 1 kcal $kg^{-1}$.°C. The enthalpy-temperature datum was taken at 0°C for both gas and liquid, and the reference states were liquid water and dry gas at the reference temperature.

The equilibrium data for $SO_2$-water system is presented in Table 2. The data were converted to mole fractions and plotted in Fig. 1 where the slopes of the equilibrium lines for pure water are 44.014, 63.321, and 86.74, respectively for temperatures between 30°C and 50°C. Fig. 2 presents the different values of the slopes of the equilibrium lines obtained at various temperatures. The solubility in pure water was based on published experimental data. The solubility of seawater TDS concentrations of 36000 and 56000 ppm were obtained experimentally [11]. The slopes corresponding to a 45000 ppm TDS used in subsequent calculates have been calculated by interpolation between the aforementioned experimental data. Thus, the slopes of the equilibrium lines for seawater at temperatures from 30°C to 50°C may be taken as 24, 34.45, and 47.2, respectively.

Table 1
Flue gas analysis

| Component | Mass fraction | Mole fraction |
|---|---|---|
| $N_2$ | 0.780159 | 0.767911 |
| $O_2$ | 0.019841 | 0.017088 |
| $SO_2$ | 0.000994 | 0.000428 |
| $NO_X$ | 0.000298 | 0.000216 |
| $CO_2$ | 0.099354 | 0.062233 |
| $H_2O$ | 0.099354 | 0.152124 |
| PM | Negligible | Negligible |
| Total | 1 | 1 |

Table 2
$SO_2$-water equilibrium data

| Mass of $SO_2$/100 masses of $H_2O$ | Partial Pressure (mmHg) | | |
|---|---|---|---|
| | 30°C | 40°C | 50°C |
| 7.5 | 688 | | |
| 5.0 | 452 | 665 | |
| 2.5 | 216 | 322 | 458 |
| 1.5 | 125 | 186 | 266 |
| 1.0 | 79 | 121 | 172 |
| 0.7 | 52 | 87 | 116 |
| 0.5 | 36 | 57 | 82 |
| 0.3 | 19.7 | | |
| 0.1 | 4.7 | 7.5 | 12.0 |
| 0.05 | 1.7 | 2.8 | 4.7 |
| 0.02 | 0.6 | 0.8 | 1.3 |

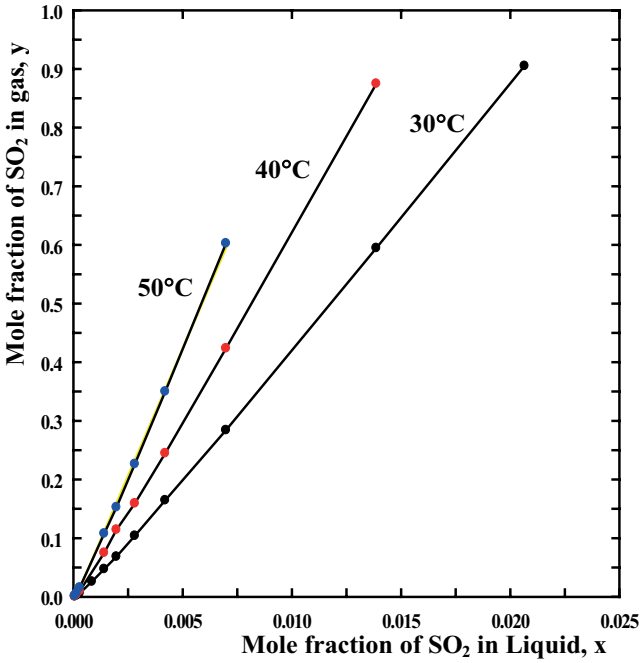


Fig. 1. $SO_2$-Water equilibrium data.

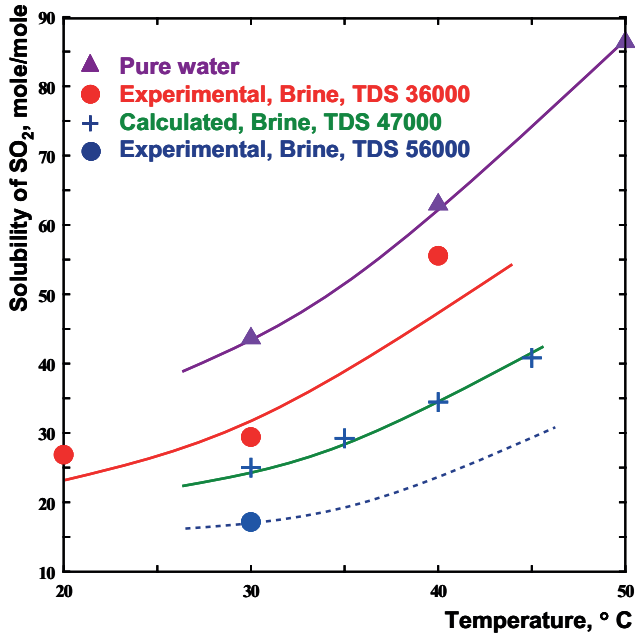


Fig. 2. $SO_2$-seawater absorption data.

*3.3. Transport parameters*

The heat transfer coefficient in the flue gas-seawater exchanger and the humid air and/or flue gas freshwater condensers were respectively, taken at $U_e$ = 55 kcal $h^{-1}.m^{-2}.°C$ and $U_c$ = 86 kcal $h^{-1}.m^{-2}$ °C [12,13]. The flue gas-air heat transfer coefficient $U_g$ was taken as 15 kcal $h^{-1}.m^{-2}$ °C [14]. The heat transfer coefficient in the counter current packed scrubber was obtained from an empirical formula which agrees well with practice and is compatible with more complicated substantiated formula:

$$k_p^{'} = 6.3\vartheta \tag{1}$$

Unlike the laboratory scale humidifier used in the experimental part, the packing in large-scale air-water contactors is made of wooden packing composed of laths laid on edge in rows and set at a certain distance from one another [14] A standard packing consists of laths of 12-mm thickness and 100-mm high-spaced 25 mm apart horizontally. In this case, 1 m of length can accommodate 27 laths; each lath has two faces with an area of 0.2 $m^2$. Therefore, 1 $m^3$ of packing would receive 54 m of irrigated ribs. The 1 m of packing will accommodate 10 rows of laths, 100 mm high, i.e., the lath total surface area/cubic meter of packing will be 54 $m^2$ $m^{-3}$ of packing. This packing occupies about 32% of the cross-sectional area leaving 68% free for gas flow. A typical mean gas velocity in the free (open) cross section of the packing is taken as 1.5 m $s^{-1}$ to avoid excessive entrainment. Therefore, $k_p$ = 510.3 kcal $h^{-1}.m^{-3}$ °C. For flue gas-water contractors, it is better to use an empty co-current configuration for the scrubber, the heat transfer coefficient in such a scrubber; increases with the spraying intensity and gas velocity and may reach up to 500 kcal $h^{-1}.m^{-3}.°C$. A more conservative figure has been estimated for the used spraying intensities in this contactor. The value of the volumetric heat transfer coefficient for this co-current contactor was set at $k_c$ = 200 kcal $h^{-1}.m^{-3}.°C$. The liquid phase and gas phase mass transfer coefficients have been correlated for each scheme according to the aforementioned absorption model.

## 4. Schemes for FGD and HDH

*4.1. Description of scheme (I)*

Scheme I is formed of flue gas-seawater exchanger and desulphurization absorber as shown in Fig. 3 Scheme I is suitable when the power stations are mainly used in conjunction with existing thermal desalination processes. The scheme consists in cooling the flue gases from a temperature of about 150°C down to 50°C in a heat exchanger against seawater, which in turn is heated from 30°C to 100°C. A minimum temperature approach of 10°C may be assumed for this exchanger. This hot seawater stream is then integrated within the existing MSF or MED process. The cooled flue gas stream is then passed through an absorber against seawater to which powdered limestone is added, if necessary, depending on the alkalinity of the seawater. The basic design models of the exchanger and absorber are here briefly outlined.

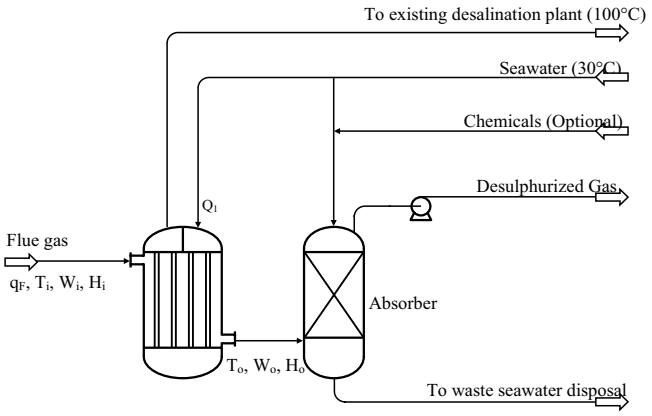


Fig. 3. Scheme (I).

*4.2. Modeling and results of scheme (I)*

*4.2.1. Flue gas–seawater exchanger*

The enthalpy loss of the flue gas within the exchanger depends on its terminal stream temperatures and humidity; thus, it is expected that some water will be condensed from the flue gas stream as it crosses the exchanger and will be mixed with the waste seawater discharged from the absorber. The inlet and outlet flue gas enthalpies are given by the following:

$$H_i = C_g T_i + (C_w T_i + \lambda) W_i \tag{2}$$

$$H_o = C_g T_o + (C_w T_o + \lambda) W_o \tag{3}$$

Thus, the quantity of water to be heated up to 100°C is calculated as:

$$Q_1 = \frac{q_F (H_i - H_o)}{C_p (100 - 30)} \tag{4}$$

The exchanger heat transfer area is obtainable in terms of the four terminal temperatures as:

$$A_e = \frac{Q_1 . C_p (100 - 30)}{U_e \Delta T_m} \tag{5}$$

where,

$$\Delta T_m = \frac{(T_o - 30) - (T_i - 100)}{Ln((T_o - 30)/(T_i - 100))} \tag{6}$$

*4.2.2. Desulphurization absorber*

The extent of purification achievable in the flue gas depends on the system's Henry's Law constant under the prevailing conditions of seawater alkalinity and temperature, the liquid to gas ratio, and the overall mass transfer coefficient. The equilibrium data are assumed to be approximately a straight line. Assuming 95% absorption of $SO_2$ in the feed

entering with composition $y_1$, the outlet gas composition would be $y_2 = 0.05\, y_1$. As seen from Fig. 4, the minimum liquid to gas ratio would be given by the following:

$$\left.\frac{L}{V}\right|_{\min} = \frac{y_1 - y_2}{(y_1/m)} \tag{7}$$

Thus, the minimum seawater solvent requirements would be given by:

$$L|_{\min} = 0.95 \times m \times V \tag{8}$$

Taking the seawater flow rate as twice the minimum value, then the absorber operating flow rate would be $L = 1.90 \times m \times V$. The absorption factor is taken at:

$$A = \frac{L}{mV} = \frac{1.90 \times m \times V}{mV} = 1.9 \tag{9}$$

The overall number of transfer units for the two schemes will be constant and calculated from the Colburn Equation [15]:

$$N_{OG} = \frac{1}{(1-1/A)} \mathrm{Ln}\left[(1-1/A)\frac{y_1 - mx_2}{y_2 - mx_2} + \frac{1}{A}\right] \tag{10}$$

Since the seawater feed is $SO_2$ free, then $mx_2 = 0$, and the number of transfer units is calculated as 4.861. The height of an overall gas phase transfer unit is obtainable from:

$$H_{OG} = \frac{V/S}{k_y' a} + \frac{1}{A}\frac{L/S}{k_x' a} \tag{11}$$

For the given liquid and gas phase molecular weights, the volumetric gas and liquid mass transfer coefficient ( $k_y' a$ ) and ( $k_x' a$ ) are given, respectively, by [15]:

$$k_y' a = 1.2482 \times \left(\frac{V}{S}\right)^{0.7} \times \left(\frac{L}{S}\right)^{0.25} \text{ and } k_x' a = 1.626 \times \left(\frac{L}{S}\right)^{0.82}$$

Therefore, $V$ and $L$ are equal to 0.0112 kmol $s^{-1}$ and 0.02128 × m, kmol $s^{-1}$, respectively. The absorber cross-sectional area, $S$ is to be calculated for each case on the basis of the anticipated pressure drop. For the two schemes, a pressure drop of 200 N $m^{-2}$ is selected. Under this condition, the packed tower curve is used, and selection of plastic pall ring packing of 3.5 in; nominal size of the corresponding value of $C_f$ is 16 [16]. The abscissa is equal to 0.041737 m and the corresponding ordinate is equal to $6.894 \times 10^{-4}$ $S^{-2}$.

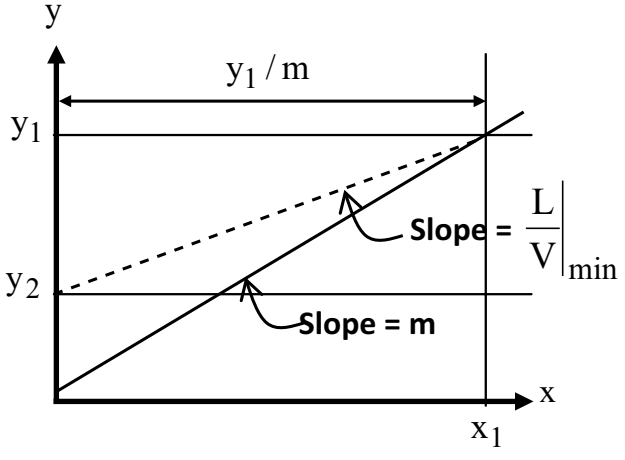


Fig. 4. Minimum seawater requirements.

A conservative value of the obtained height considering the uncertainties in the mass transfer correlations would be obtained by multiplying the height by a factor of 2. Table 3 summarizes the results of the design calculations for scheme (I).

The constraints of inlet and outlet temperatures leave no room for changing the design duty of the heat exchanger. It is designed on the basis of maximizing the heat recoverable from the flue gas and keeping the exit water temperature below 100°C to avoid evaporation in the exchanger. The desulphurization unit is optimized by striking a balance between the purification required on one hand and the liquid to gas ratio and contactor size on the other.

### 4.3. Description of scheme (II)

As shown in Fig. 5, this scheme consists in cooling the flue gases down to 50°C, and subsequently, treating the flue gas in an absorption unit. The hot seawater leaving the exchanger is then contacted in a humidifier with an air stream recirculating between the humidifier and a surface dehumidification condenser. Seawater is used as the cooling medium in this condenser, and part of the effluent cooling seawater at a temperature of about 40°C is used in the flue gas cooling heat exchanger. This scheme is addressed to situations where the power station is not associated with a desalination plant.

### 4.4. Model and results of scheme (II)

#### 4.4.1. Exchanger seawater

It is similar to scheme (I), but is based on recovering desalinated water from the hot seawater stream through a humidification dehumidification desalination system. The feed seawater to the cooling exchanger would be at 40°C rather than at 30°C; therefore, the cooled flue gas temperature will be 50°C rather than 40°C.

#### 4.4.2. The air humidifier

The sensible heat in the heated seawater stream leaving the exchanger is partly recovered in humidifying a re-circulating air stream. Allowing a temperature approach of 10°C in the dehumidification condenser, the air stream leaving the condenser is assumed at 40°C, since the maximum seawater

Table 3
Scheme (I) results

| Parameter | Values |
|---|---|
| Product hot water ($Q_1$ kg $h^{-1}$) | 997.218 |
| Required exchanger area ($A_e$ $m^2$) | 51.07184 |
| Required absorber seawater (L, kg $h^{-1}$) | 40299.64 |
| Required absorber height (m) | 3.056 |

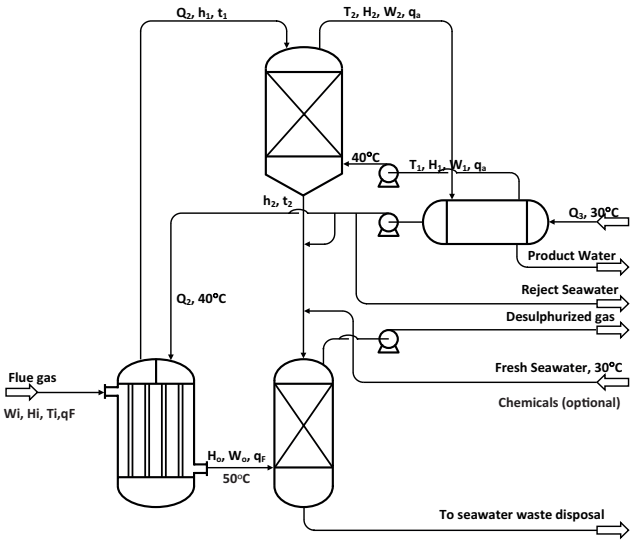


Fig. 5. Scheme (II).

temperature is estimated at 30°C. The enthalpies of the hot water and air entering the humidifier are respectively, given by the following:

$$h_1 = Q_2 C_p t_1 \tag{12}$$

$$H_1 = q_a(C_g T_1 + (C_w T_1 + \lambda)W_1) \tag{13}$$

While, the enthalpies of the liquid and air streams leaving the unit are respectively, given by:

$$h_2 = (Q_2 - q_a(W_2 - W_1))C_p t_2 \tag{14}$$

$$H_2 = q_a(C_g T_2 + (C_w T_2 + \lambda)W_2) \tag{15}$$

In order to recover as much as possible of freshwater in the humidified air, the condenser air exit temperature will be set as previously explained at 40°C. The humidifier acts as a cooling tower. A wooden slat forced draft contactor design is appropriate for the aforementioned operating conditions. It is reasonable to set the exit water temperature at 50°C to provide for a 10°C temperature approach at the bottom of the humidifier. It is to further assume that the air stream entering the humidifier is saturated, and that the air stream leaving the humidifier is at 95% relative saturation.

For a given air stream flow rate, the heat balance equation is formulated by combination of Eqs. (12)–(15):

$$h_1 + H_1 = h_2 + H_2 \tag{16}$$

This can be reduced to:

$$Q_2 C_p t_1 + q_a(C_g T_1 + (C_w T_1 + \lambda)W_1) = (Q_2 - q_a(W_2 - W_1))C_p t_2 + q_a(C_g T_2 + (C_w T_2 + \lambda)W_2) \tag{16'}$$

Eq. (16) would involve two unknowns, namely, $T_2$ and $W_2$; since the humid air is assumed to be saturated, i.e., $W_1$=$W_s$:

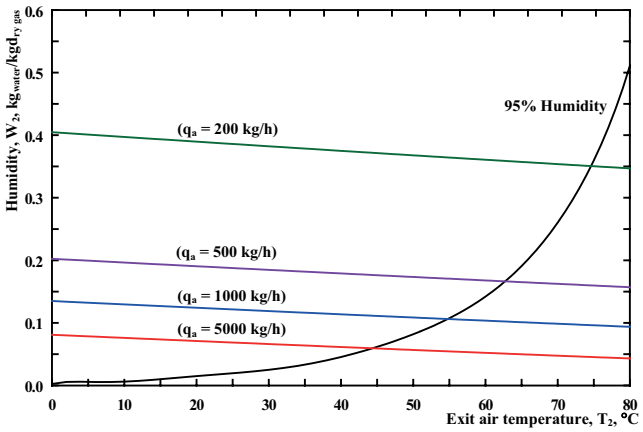


Fig. 6. Determination of humidifier exit air conditions.

Table 4
Effect of air flow rate on humidifier performance

| Air ($q_a$, kg h$^{-1}$) | $T_2$ (°C) | $W_2$ (kg kg$^{-1}$) | $M_w$ (kg h$^{-1}$) |
|---|---|---|---|
| 5000 | 44.3656 | 0.059305 | 55.025 |
| 2500 | 47.4312 | 0.070854 | 56.385 |
| 1500 | 51.0092 | 0.086416 | 57.174 |
| 1000 | 54.7829 | 0.106097 | 57.797 |
| 500 | 62.7197 | 0.166289 | 58.9945 |
| 400 | 65.5148 | 0.196773 | 59.3892 |
| 300 | 69.2329 | 0.247857 | 59.8671 |
| 200 | 74.6156 | 0.350548 | 60.4496 |

$$W_2(T) = 0.95\frac{P(T)}{\pi - P(T)}\frac{M_w}{M_g} \tag{17}$$

The simultaneous solution of the enthalpy balance Eq. (16) and the temperature saturation humidity Eq. (17) give the exit air temperature $T_2$.

From a process design point of view, various values of $q_a$ are assigned. For each value of $q_a$, Eq. (16) reduces to a relation between the temperature and humidity of the humidifier effluent air. Since this is assumed 95% saturated, the solution of this equation with the 95% relative saturation-temperature data based on water vapor pressure data (Eq. 17) would give $T_2$ and $W_2$ as illustrated in Fig. 6.

The 95% saturation humidity-temperature data have been calculated from Eq. (17) and fitted to a ninth order polynomial to be solved simultaneously with Eq. (16). The calculations assumed a range of ($q_a$) from 200 to 5,000 kg h$^{-1}$ and are presented in Table 4 and in Figs. 7 and 8.

The volume of the humidifier is calculated from Eq. (18) where $k_p$ = 500 kcal h$^{-1}$.m$^{-3}$.°C. The difference between the inlet and outlet water heat contents ($h_1$–$h_2$) depends on the amount of water evaporated in the humidifier; also, $\Delta T_m$ depends on the exit air temperatures corresponding to the various air flow rates. Table 5 summarizes the values of $\Delta T_m$, and $Q_3(h_1 - h_2)$ as a function of the dry air recirculation rate, and the corresponding value of the required humidifier volume which is also shown in Fig. 9.

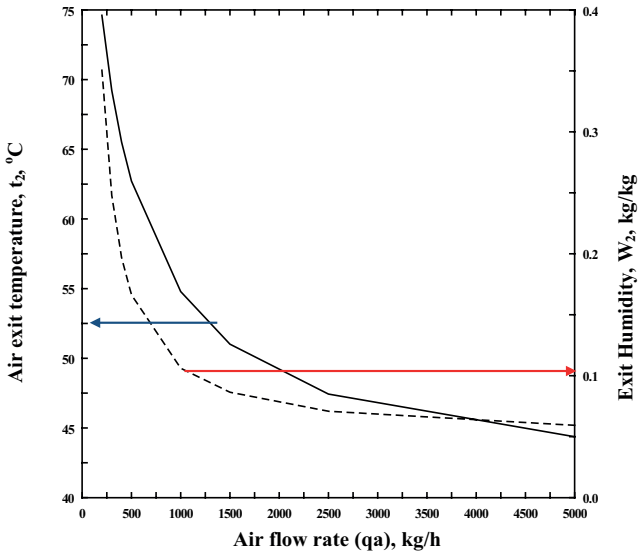


Fig. 7. Effect of air flow rate on its exit temperature and humidity.

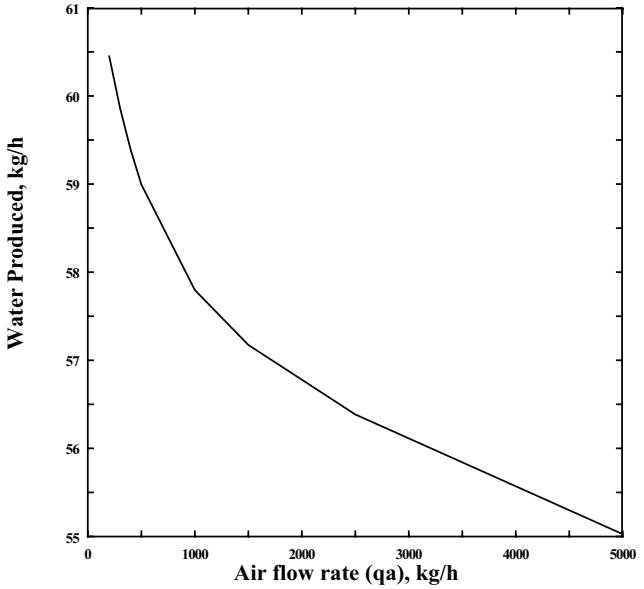


Fig. 8. Effect of air flow rate on the amount of water produced.

Table 5
Volume of humidifier

| $q_a$(kg h$^{-1}$) | $\Delta T_m$ (°C) | $h_1 - h_2$ | Volume (m$^3$) |
|---|---|---|---|
| 5000 | 26.59012 | 39678.84 | 2.98448 |
| 2500 | 25.651 | 39746.84 | 3.099048 |
| 1500 | 24.53722 | 39786.29 | 3.242934 |
| 1000 | 23.33974 | 39817.44 | 3.411987 |
| 500 | 20.7316 | 39877.32 | 3.847007 |
| 400 | 19.77891 | 39897.05 | 4.034303 |
| 300 | 18.47834 | 39920.95 | 4.320836 |
| 200 | 16.51485 | 39950.07 | 4.83808 |

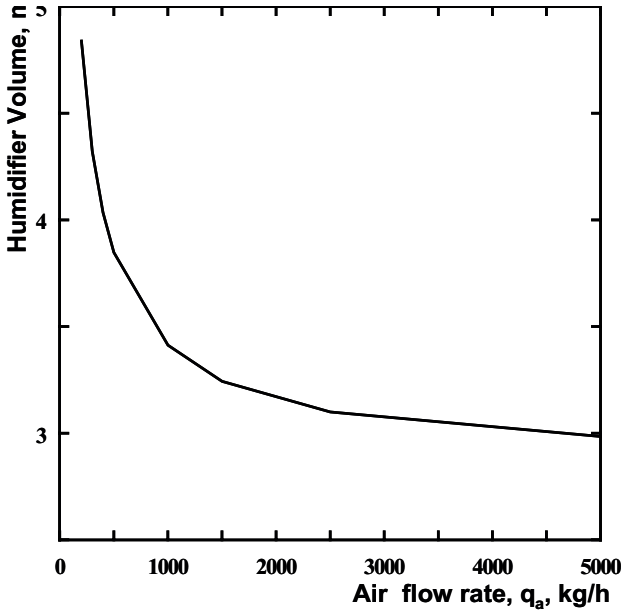


Fig. 9. Variation of humidifier volume with air flow rate.

It is to be noticed that since a velocity of 1.5 m s$^{-1}$ is assumed for the gas stream in the open packing cross section, the cross-sectional area required on the basis of 1,000 kg h$^{-1}$ dry flue gas will increase with the air recirculation rate.

Given the water stream enthalpy loss and the four terminal stream temperatures, the volume of the dehumidifier is obtained from:

$$v_p = \frac{h_1 - h_2}{k_p . \Delta T_m} \tag{18}$$

$$\Delta T_m = \frac{(t_1 - T_2) - (t_2 - T_1)}{\mathrm{Ln}((t_1 - T_2)/(t_2 - T_1))} \tag{19}$$

*4.4.3. Freshwater condenser*

The amount of freshwater produced in the condenser is obtained from the humidity differences of the in and out air streams; thus, the amount of fresh water produced, $F$ is obtained from:

$$F = q_a(W_2 - W_s) \tag{20}$$

The condenser heat load is calculated as the difference between the inlet and outlet air enthalpies. This enables the required cooling water rate to be calculated by assuming a 10°C temperature rise, i.e., an exit seawater temperature of 40°C. Thus,

$$Q_3 = \frac{q_a(H_2 - H_1)}{C_p(40 - 30)} \tag{21}$$

The heat transfer surface is thus obtained as:

$$A_c = \frac{q_a(H_2 - H_1)}{U_c \Delta T_m} \tag{22}$$

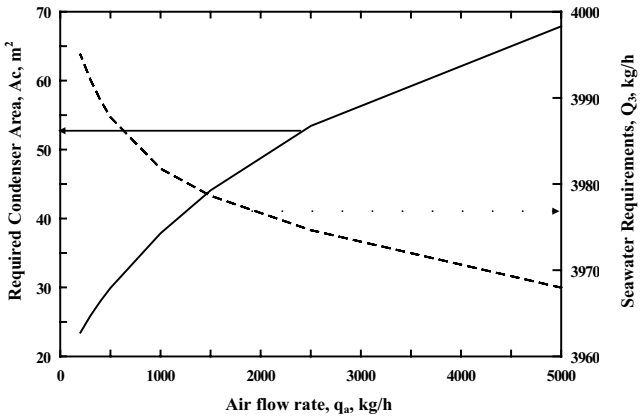


Fig. 10. Condenser area and seawater requirements vs. circulating air.

$$\Delta T_m = \frac{(T_2 - 40) - (T_1 - 30)}{Ln((T_2 - 40)/(T_1 - 30))} \quad (23)$$

Fig. 10 shows the variation of the seawater requirements vs. the air flow rate. The required area of condenser also varies with the air requirements; it is calculated from Eq. (22) and is also presented in Fig. 10.

The indirect heat exchange between the flue gases and seawater is similar to that in scheme (I) except that the inlet seawater temperature would be at about 40°C rather than at 30°C. This fixes the amount of water to be heated to 100°C, as well as the heat exchanger surface. As for the humidifier, the choice of the re-circulated air volume affects the exit air temperature and humidity, as well as the size of the humidifier. These would in turn affect the cooling water requirements and the heat transfer surface required for the freshwater condenser.

#### *4.4.4. Desulphurization absorber*

Since larger quantities of seawater will be required for cooling, exceeding the humidification requirements, part of the condenser exit seawater is used for the flue gas absorption in order to save some of the seawater pumping power requirements. This water would be at 40°C rather than at 30°C, as was the case with scheme (I). Also, since a minimum temperature approach of 10°C has been set for the cold end of the exchanger, the flue gas entering the absorber would be at 50°C rather than at 40°C. This would be reflected on the size of the desulphurization absorption tower, unless some ways of further alkalization of the seawater are provided for.

It is clear that as the air recirculation rate is increased, the humidifier volume decreases; while the required heat transfer surface in the condenser increases. Since the cost per unit area of the condenser is higher than the cost per unit volume of the humidifier, it is better to select a small air re-circulation rate. This would also correspond to a smaller cross section of the humidifier and smaller air re-circulation power requirements. On the other hand, the liquid-to-air ratio should be maintained within a suitable range to avoid excessive entrainment.

Taking the air flow rate at 500-kg $h^{-1}$ dry air, the humidity of the entering air is 0.0483 and that of the exit air is 0.166289; therefore, the average humidity within the humidifier, Wav is 0.1073. The average temperature, $T_{av}$ is 51.35985°C; therefore, the average humid volume per kilogram dry air maybe calculated from:

$$v_w = (0.082 \times T_{av} + 22.41)\left(\frac{1}{M_g} + \frac{W_{av}}{M_w}\right) \quad (24)$$

This gives the average volumetric flow rate 500 × 1.068 = 534 $m^3 h^{-1}$ which can pass through 68% of the total cross-sectional area. The required humidifier area would be 0.1454 $m^2$/1,000-kg $h^{-1}$ dry air. This corresponds to a spraying intensity of 1.38 $m^3$ of water/1,000 $m^3$ of re-circulating air, or 5.08 $m^3$ of water/h $m^{-2}$ of tower cross section. Table 6 summarizes the results of the design calculations for scheme (II).

Table 6
Scheme (II) results

| Parameter | Values |
|---|---|
| Flue gas exchanger seawater ($Q_2$ kg $h^{-1}$) | 738.5518 |
| Required exchanger area ($A_e$, $m^2$) | 32.41834 |
| Amount of re-circulating air ($q_a$, kg $h^{-1}$) | 500 |
| Condenser cooling seawater ($Q_3$ kg h0$^{-1}$ | 3987.751 |
| Required condenser area ($A_c$ $m^2$) | 29.91639 |
| Product water (kg $h^{-1}$) | 58.9945 |
| Humidifier volume ($m^3$) | 3.847007 |
| Humidifier area ($m^2$) | 0.1454 |
| Required absorber seawater (L, kg $h^{-1}$) | 56295.39 |
| Required absorber height (m) | 3.000778 |

## 5. Comparison of the two schemes

The design calculations for the scheme (I) included the calculation of the amount of hot seawater obtainable at 100°C on cooling the flue gas from 150°C down to 40°C. Summaries of the results of the design calculations for schemes (I) and (II) and the equipment required for the integration of FGD and HDD schemes are presented in Table 7. It is worth noting that in scheme (I), no freshwater is produced, but a hot seawater stream at 100°C can be sent to an existing desalination unit. The calculations of the different equipment sizing are based on a dry flue gas rate of 1,000 kg $h^{-1}$ at 150°C, and the analysis is given in Table 1.

## 6. Conclusions

This study was focused on modeling and analysis of the integration of FGD and HDD. Two alternative schemes were proposed, modeled and, compared for the integration between FGD and sea water desalination. The process design calculations were based on reliable overall heat and mass transfer coefficient data. The analysis included sizing

Table 7
Comparison of the two schemes

| Parameter | Scheme (I) | Scheme (II) |
|---|---|---|
| Flue gas exchanger area ($A_e$, m$^2$) | 51.07184 | 32.41834 |
| Required humidifier (m$^3$) | — | 3.847007[a] |
| Air recirculation rate (kg h$^{-1}$) | — | 500 |
| Cooling seawater in condenser, (m$^3$ h$^{-1}$) | — | 3.987 |
| Condenser water to humidifier, (m$^3$ h$^{-1}$) | — | — |
| Condenser area $A_c$ (m$^2$) | — | 29.91639 |
| Product freshwater ($Q_1$, kg h$^{-1}$) | 332[b] | 58.995 |
| Purity of freshwater | Pure | Pure |
| Required absorber seawater (L, kg h$^{-1}$) | 40299.64 | 56295.39 |
| Absorber area (m$^2$) | 0.2626 | 0.313824 |
| Absorber height (m) | 3.056 | 3.000778 |

[a]volume of packing.
[b]997.218 kg h$^{-1}$ of hot seawater at 100°C is to be directed to desalination plant.

of the required HDD units, evaluation of the specific amount of water generated relative to the plant power capacity, and the design characteristics and the performance of the seawater absorption column for $SO_2$ removal from the flue gases. Laboratory scale preliminary set of experiments were compared with available data on the mass transfer coefficients for $SO_2$ absorption in seawater and the overall heat transfer coefficients in packed air humidification contacting towers.

Scheme (I) would be preferred if burning sulfurous fuels are used in conjunction with MSF or MED plants. Cooling of the flue gas (prior to desulfurization)could result in a credit hot seawater stream to be integrated with the existing desalination unit. Scheme (II) relies on air humidification. The air is humidified by hot water ensuing from the flue gas heat exchanger. It involves less heat transfer surfaces in the heat exchanger and surface condenser. Scheme (II) requires larger towers compared to scheme (I). For scheme (II), the amount of water produced per unit area of heat transfer surface is 0.9465.

The proposed models can be applied to the operating conditions of the power plants in Kuwait. This is motivated by the large capacity of these plants, the use of high sulfur oil fuels, and the need for reducing the greenhouse gases which contribute to global climate change.

## Nomenclature

$y$ — Mole fraction of $SO_2$ in gas phase
$x$ — Mole fraction of $SO_2$ in liquid phase
$\vartheta$ — Mean gas velocity in the open cross section of the contactor
$T_s$ — Adiabatic saturation temperature, °C
$q_a$ — Air recirculation rate on a dry basis, kg h$^{-1}$
$W$ — Humidity, kg water/kg dry air
$T_{av}$ — Average temperature within the humidifier, °C
$q_f$ — Dry flue gas rate, kg h$^{-1}$
$Hi,o$ — Inlet and outlet flue gas enthalpies
$H_4$ — Enthalpy/kilogram dry air leaving the exchanger assumed at 130°C
$\rho_G$ — Flue gas density, 1.13 kg m$^{-3}$
$T$ — Temperature, °C
$\lambda_S$ — Heat of vaporization at 60°C = 564.196 kcal kg$^{-1}$
$v_w$ — Humid volume, m$^3$ kg$^{-1}$
$c$ — Seawater concentration, $kg_{salt}/kg_{seawater}$
$a$ — Interfacial area per unit volume
$V'$ — Mass velocity of flue gas, kg s$^{-1}$.m$^2$
$L'$ — Mass velocity of seawater, kg s$^{-1}$.m$^2$
$U$ — Over heat transfer coefficient, kcal h$^{-1}$.m$^2$.°C
$C_f$ — Parameter depending on type and size of packing
$W_s$ — Saturation humidity kg, water kg$^{-1}$ dry flue gas
$\rho_L$ — Seawater density, 1,000 kg m$^{-3}$
$\pi$ — Total pressure
$\mu_L$ — Viscosity of seawater taken at kg m$^{-1}$.s.
$v_s$ — Volume of the required empty scrubber, m$^3$
$k_p$ — Volumetric heat transfer coefficient in the packed section, kcal h$^{-1}$.m$^3$.°C
$k'_p$ — Heat transfer coefficient in the packed section, kcal h$^{-1}$.m$^3$.°C
$\nu_p$ — Volume of the required wooden lath packed section
L — Seawater flow rate, kmole s$^{-1}$
$M_g$ — Molecular weight of flue gas
$M_w$ — Molecular weight of water
$P(T)$ — Vapor pressure of water at temperature, $t$
S — Cross-sectional area of column
V — Flue gas flow rate, kmole s$^{-1}$

## References

[1] B. Everett, G. Alexander, Working with our environment, energy file part 1A: energy and its use, Energy Sources, 1 (2002) 5–6.
[2] S. Alotaibi, Energy consumption in Kuwait: prospects and future approaches, Energy Policy, 39 (2011) 637–643.
[3] M.A. Darwish, N. Al-Najem, The water problem in Kuwait, Desalination, 177 (2005) 167–177.
[4] M.A. Darwish, S. Alotaibi, S. Alfahad, On the reduction of desalting energy and its cost in Kuwait, Desalination, 220 (2008) 183–495.
[5] A. Alhaddad, H. Ettouney, S. Saqer, Analysis of air pollution emission patterns in the vicinity of oil refineries in Kuwait, J. Eng. Res., 3 (2015) 1–24.
[6] J. Cohen, I. Janovich, A. Muginstein, Utilization of waste heat from a flue gases up-stream gas scrubbing system, Desalination, 139 (2001) 1–16.
[7] M. Cohen, I. Ianovici, D. Breschi, Power plant residual heat for seawater desalination, Desalination, 152 (2003) 155–165.
[8] H. Ettouney, Design and analysis of humidification dehumidification desalination process, Desalination, 183 (2005) 341–352.
[9] G. Al-Enezi, H. Ettouney, N. Fawzy, Low temperature humidification dehumidification desalination, Energy Convers. Manage., 47 (2006) 470–484.
[10] R.S. Ettouney, N. Fawzy, M.A. El-Rifai, H. Ettouney, Flue gas desulfurization and humidification dehumidification in power plants, Desal. Water Treat., 37 (2012) 337–349.
[11] G. Al-Enezi, H. Ettouney, H. El-Dessouky, N. Fawzy, Solubility of sulfur dioxide in seawater, Ind. Eng. Chem. Res., 40 (2001) 1434–1441.

[12] M. Farid, S. Parekh, J.R. Selman, S. Al-Hallaj, Solar desalination with a humidification-dehumidification cycle: mathematical modeling of the unit, Desalination, 151 (2002) 153–164.
[13] R.H. Xiong, S.C. Wang, L.X. Xie, Z. Wang, P.L. Li, Experimental investigation of a baffled shell and tube desalination column using the humidification-dehumidification process, Desalination, 180 (2005) 253–261.
[14] G.Gordon, L. Peisakhov, Dust Collection and Gas Cleaning, MIR Publishers: Moscow, 1972, pp. 211–435.
[15] C.J. Geankopolis, Transport Processes and Unit Operations, 4th ed., 1993, pp. 616–677.
[16] R.E. Treybal, Mass-Transfer Operations, 3rd ed., 1980, pp. 195–250.